

Flexural performance of wooden beams strengthened by composite plate

Hassaine Daouadji Tahar*, Rabahi Abderezak and Benferhat Rabia

*Department of civil engineering, Laboratory of Geomatics and sustainable development,
University of Tiaret, Algeria*

(Received April 23, 2020, Revised July 13, 2020, Accepted September 8, 2020)

Abstract. Using bonded fiber-reinforced polymer laminates for strengthening wooden structural members has been shown to be an effective and economical method. In this research, properties of suitable composite materials (sika wrap), adhesives and two ways of strengthening beams exposed to bending moment are presented. Passive or slack reinforcement is one way of strengthening. The most effective way of such a strengthening was to place reinforcement laminates in the stretched part of the wooden beam (lower part in our case), in order to investigate the effectiveness of externally bonding FRP to their soffits. The model is based on equilibrium and deformations compatibility requirements in and all parts of the strengthened beam, i.e., the wooden beam, the sika wrap composite plate and the adhesive layer. The theoretical predictions are compared with other existing solutions. This research is helpful for the understanding on mechanical behaviour of the interface and design of the composite-wooden hybrid structures. The results showed that the use of the new strengthening system enhances the performance of the wooden beam when compared with the traditional strengthening system.

Keywords: composite plate; interfacial stresses; wooden beam; strengthening, shear lag effect

1. Introduction

The interest of the construction is to build structures which must resist the loads which are subjected to them in order to fulfill a function (to accommodate people, to allow vehicles to cross a watercourse, etc) but these structures must also resist environmental damage and be sustainable over time. The objective is that the structure keeps the same level of performance for as long as possible: ability to distribute loads, durability vis-à-vis the outside environment, aesthetic appearance. If the level of performance drops, the structure must be strengthened: this is the principle of renovation. In wood construction, a new technology is emerging to increase the resistance of structures: these are CFRP (Carbon Fibers Reinforced Polymers), polymers reinforced by carbon fibers. The advantage of this application is that it can be used both during the construction of a structure and during its renovation (Abdelhady *et al.* 2006, Benachour *et al.* 2008, Liu *et al.* 2019, Panjehpour *et al.* 2016, Chaabane *et al.* 2019, Chikr *et al.* 2020, Draiche *et al.* 2019, Hussain *et al.* 2020, Rabahi *et al.* 2019, Daouadji 2013, Yehia *et al.* 2018, Wang *et al.* 2020 and Zidour *et al.* 2020). This technology is already used in reinforced concrete structures.

*Corresponding author, Professor, E-mail: daouadjitahar@gmail.com

Wood-based beams, such as solid structural timber, glued laminated timber or other engineering wood products might need strengthening in existing structures such as floors, roofs, industrial girders or even timber bridges for several reasons such as increase in service loads or degradation of the material. Sometimes newly designed timber structures could be more price-competitive if the height of the structural members was minimized. Examples of such members are column and beam systems (in multi-storey buildings) and timber bridges where the total construction height of beams and deck can be of significant importance. In order to obtain a large contribution of sika wrap (FRP) strengthening in load bearing capacity, a large transfer of force to composite laminate is necessary (Hassaine Daouadji 2017, Abualnour *et al.* 2019, Alimirzaei *et al.* 2019, Al-Furjan *et al.* 2020, AliShariati *et al.* 2020, Belbachir *et al.* 2020, Benhenni *et al.* 2019, Bensattalah *et al.* 2018, Bekki *et al.* 2019, Chaded *et al.* 2018, Tahar *et al.* 2019, Boutaleb *et al.* 2019, Bousahla *et al.* 2020, Bourada *et al.* 2020, Abdederak *et al.* 2018, Abdelhak *et al.* 2016, Adim *et al.* 2018, Benferhat *et al.* 2019, Pello *et al.* 2020, Robert *et al.* 2016, Smith and Teng 2002 and Tounsi *et al.* 2008). Study of the force transfer mechanism in adhesive joints shows that a large portion of the force is normally transferred at a rather short distance at the ends of the laminate referred to as anchorage length. The larger the difference between the modulus of elasticity of timber and composite material, the higher the force carried by the composite laminate which leads to higher shear stresses along the anchorage length in the adhesive layer and the wooden substrate. Due to the limited shear strength of wood and tension perpendicular to the grain, the failure of composite bonded timber members is usually governed by debonding of the composite laminate at timber material level, subject of this study.

Proper selection and application of the adhesive will ensure that debonding due to cohesion or adhesion failure does not occur. Debonding reduces the utilization of the composite laminate and is usually characterized by separation of the strengthening laminate from the structural member. This is the same case for reinforced concrete beams where several researchers have well studied this phenomenon of detachment of the composite plate (separation of the sika wrap composite plate) often called the shear lag effect (Amara *et al.* 2019, Chaded *et al.* 2018, Hassaine Daouadji 2008, Guenaneche *et al.* 2014 Kaddari *et al.* 2020, Benferhat *et al.* 2018, Benhenni *et al.* 2018, Karami *et al.* 2019, Matouk *et al.* 2020, Rabhi, M., *et al.* 2020, Rahmani *et al.* 2020, Refrafi *et al.* 2020, Sahla *et al.* 2019, Tahar *et al.* 2013, Tayeb *et al.* 2020, Shariati *et al.* 2020, Tounsi *et al.* 2020, Chergui *et al.* 2019, Rabahi *et al.* 2018 and Yuan *et al.* 2019). The transferring of stresses from wood to the composite is central to the effect of composite-strengthened wood structures. This is because these stresses are likely to cause undesirable premature and brittle failure. In strengthening reinforced wooden beams with composite strips, different failure modes have been observed. Generally speaking, there exist four distinct failure modes (Hugo *et al.* 2017) as described in see in Fig. 1.

One main disadvantage is the risk of premature debonding of the composite from the substrate, which is a serious hindrance for the success of the bonding technique. For uniformly distributed load (q) four classical rupture modes should be guaranteed, Fig. 1 show four possible situations in which premature rupturing of timber beams (Hugo *et al.* 2017) can occur:

- 1) Rupture of composite strips, the composite plate rupture at the ultimate strain,
- 2) The crushing of the timber in the regions subjected to compression stresses. The former is most unlikely to occur unless additional mechanical anchorages are used and applied at both ends of the composite, whereas the latter may occur when an exaggerated amount of composite is used and the shear strength of the timber is not exceeded,
- 3) Shear crack due to an insufficient bonding anchorage length, flexure crack induced interfacial debonding,
- 4) Delamination of composite strips, the delamination of composite plate occurs rather

catastrophically in an unstable manner, the crack initiates from the end of the composite strips or the bottom of a flexural or shear/flexural crack in the wooden beam member. One is due to the strains in the composite that reach a value much lower than the rupture strain limit, which represents a waste of composite material used in the repair or strengthening of the timber element. The other is the reduced load-carrying capacity of the timber beams flexural strengthened with composites due to one of those premature rupture modes.

The present paper is devoted to understanding the mechanism of debonding failure mode and the development of sound design rules. This brittle mode of failure is a result of the high shear and vertical normal (peeling) stress concentrations arising at the edges of the bonded composite plate (this is the fourth case of Fig. 1, that of the detachment of the composite plate at the end of the composite free end). Hence, this limited area in the close vicinity of the bonded strip edge, subjected to high peeling and interfacial shear stresses, proves to be among the most critical parts of the strengthened beams. Consequently, the determination of interfacial stresses has been researched for the last decade for beams bonded with either advanced composite materials. Recommendations and conclusions will be drawn after analysis and modeling of the proposed model. Most of the research efforts have focused on strengthening of RC beams with externally bonded sheets, whereas the interfacial stresses in wooden beams strengthened by externally bonded FRP strips has not been fully studied yet.

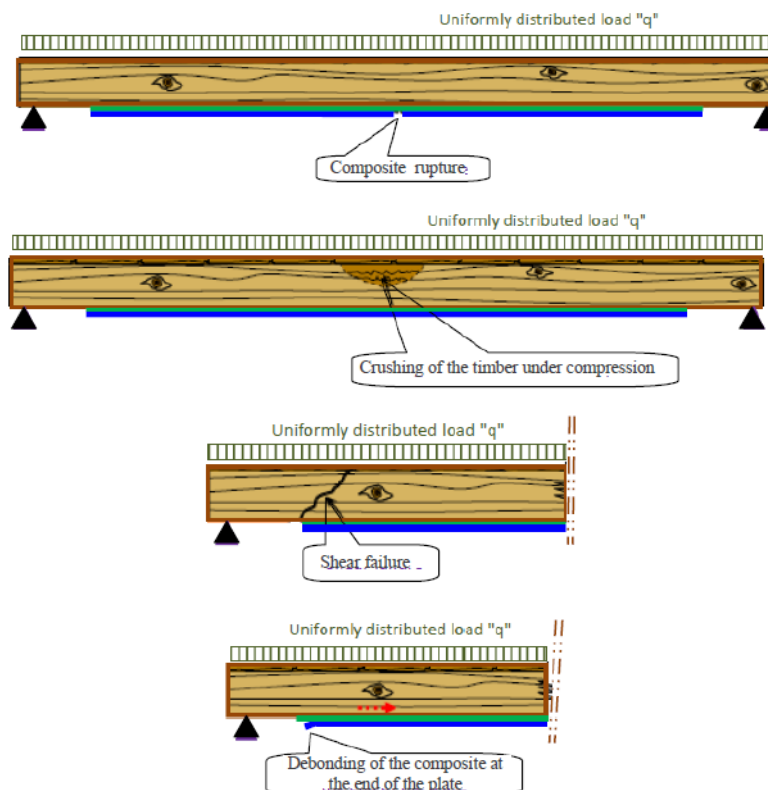


Fig. 1 Different type of rupture mode in wooden beams strengthened with composites

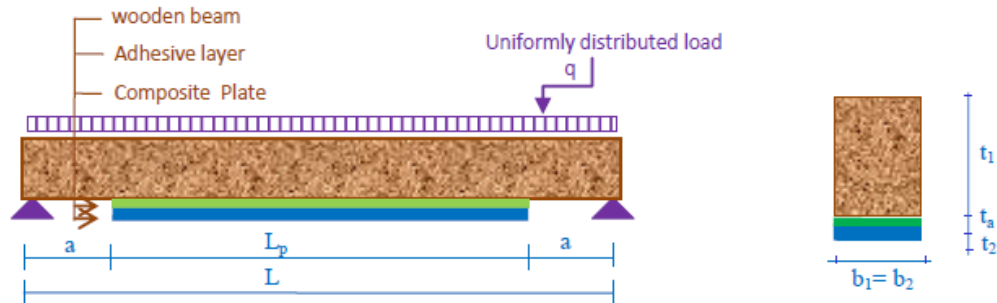


Fig. 2 Simply supported wooden beam strengthened bonded with composite plate

The main objective of the present study is to analyze the interfacial stresses in wooden beams strengthened with sika wrap composite plate. The simple approximate closed-form solutions discussed in this paper provide a useful but simple tool for understanding the interfacial behaviour of an externally bonded composite plate on the wooden beam.

2. Theoretical formulation and solutions procedure

2.1 Assumptions of the new solution

The present analysis takes into consideration the transverse shear stress and strain in the beam and the plate but ignores the transverse normal stress in them. One of the analytical approach proposed by Hassaine Daouadji *et al.* (2016) for concrete beam strengthened with a bonded FRP Plate was used in order to compare for the present model (wooden beam bonded by composite) it with another analytical models (Fig. 2).

The analytical approach (Hassaine Daouadji *et al.* 2016) is based on the following assumptions:

- Elastic stress strain relationship for composite and adhesive;
- There is a perfect bond between the composite plate and the wooden beam;
- The adhesive is assumed to only play a role in transferring the stresses from the wooden beam to the composite plate reinforcement;
- The stresses in the adhesive layer do not change through the direction of the thickness.

Since the composite laminate is an orthotropic material, its material properties vary from layer to layer. In analytical study (Hassaine Daouadji *et al.* 2016), the laminate theory is used to determine the stress and strain behaviours of the externally bonded composite plate in order to investigate the whole mechanical performance of the composite – strengthened structure. The laminate theory is used to estimate the strain of the symmetrical composite plate.

2.2 Basic equation of elasticity

A differential section dx , can be cut out from the composite wooden beam, as shown in Fig. 3. The composite beam is made from three materials: wooden, adhesive layer and composite reinforcement.

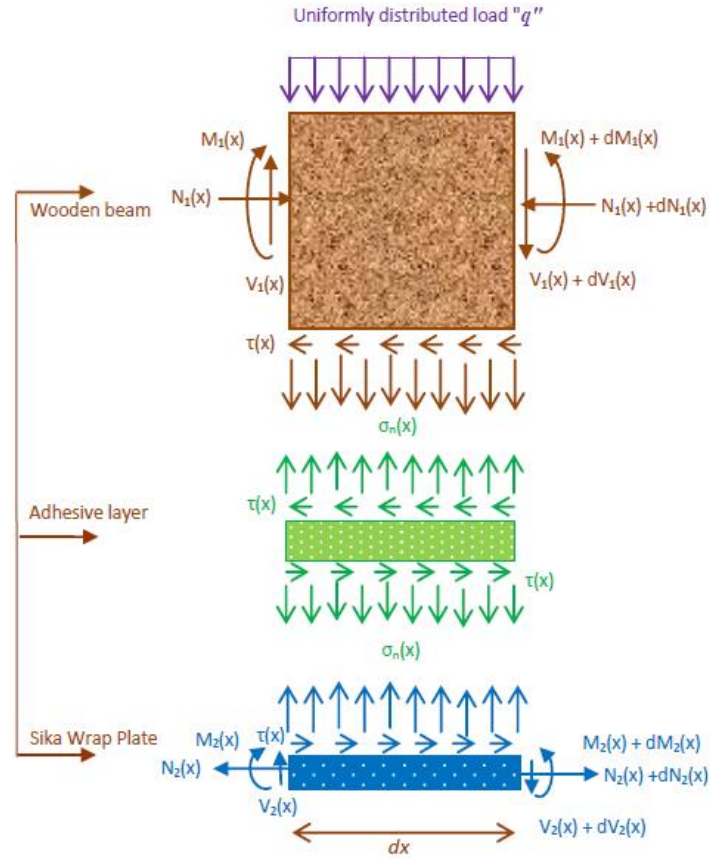


Fig. 3 Forces in infinitesimal element of a soffit-plated beam

In the present analysis, linear elastic behaviour is regarded to be for all the materials; the adhesive is assumed to play a role only in transferring the stresses from the wooden to the sika wrap reinforcement and the stresses in the adhesive layer do not change through the direction of the thickness.

The strain $\epsilon_1(x)$ in the wooden beam near adhesive interface ($y_1 = t_1/2$) can be expressed as

$$\epsilon_1(x) = \frac{du_1(x)}{dx} = \frac{y_1}{E_1 I_1} M_1(x) - \frac{N_1}{E_1 A_1} + \frac{t_1}{4G_1} \frac{d\tau_a}{dx} \tag{1}$$

The laminate theory is used to estimate the strain $\epsilon_2(x)$ in the external composite reinforcement near adhesive interface. Furthermore, it is assumed that the ply arrangement of the plate is symmetrical.

$$\epsilon_2(x) = \frac{du_2(x)}{dx} = A_{11}' \frac{N_2(x)}{b_2} - D_{11}' \frac{t_2}{2b_2} M_2(x) \tag{2}$$

where $u_1(x)$ and $u_2(x)$ are horizontal displacements of the wooden and the external sika wrap reinforcement near interface, respectively; $M_1(x)$ and $M_2(x)$ are bending moments applied in the wooden and the external composite (sika wrap) reinforcement, respectively; E_1 is Young's modulus of the wooden beam; I_1 is the second moment area; e is distance from the neutral axis to the bottom of wooden beam; N_1 and N_2 are axial forces applied in the wooden and the external composite (sika wrap) reinforcement, respectively; b_2 is the width of the plate; t_2 is thickness of the external reinforcement; $[A'] = [A^{-1}]$ is the inverse of the extensional matrix $[A]$; and $[D'] = [D^{-1}]$ is the inverse of the flexural matrix, explicitly the terms of the matrices $[A]$ and $[D]$ are written as:

Extensional matrix

$$A_{ij} = \sum_{k=1}^{n_l} \bar{Q}_{ij}^k ((y_2)_k - (y_2)_{k-1}) \quad (3)$$

Flexural matrix

$$D_{ij} = \frac{1}{3} \sum_{k=1}^{n_l} \bar{Q}_{ij}^k ((y_2^3)_k - (y_2^3)_{k-1}) \quad (4)$$

The subscript n_l represents the number of laminate layers of the composite (sika wrap) plate, \bar{Q}_{ij} can be estimated by using the off-axis orthotropic plate theory, where

$$\bar{Q}_{11} = Q_{11} m^4 + 2(Q_{12} + 2Q_{33})m^2 n^2 + Q_{22} n^4 \quad (5)$$

$$\bar{Q}_{12} = (Q_{11} + Q_{22} - 4Q_{33})m^2 n^2 + Q_{12}(n^4 + m^4) \quad (6)$$

$$\bar{Q}_{22} = Q_{11} n^4 + 2(Q_{12} + 2Q_{33})m^2 n^2 + Q_{22} m^4 \quad (7)$$

$$\bar{Q}_{33} = (Q_{11} + Q_{22} - 2Q_{12} - 2Q_{33})m^2 n^2 + Q_{33}(n^4 + m^4) \quad (8)$$

And

$$Q_{11} = \frac{E_1}{1 - \nu_{12} \nu_{21}} \quad (9)$$

$$Q_{22} = \frac{E_2}{1 - \nu_{12} \nu_{21}} \quad (10)$$

$$Q_{12} = \frac{\nu_{12} E_2}{1 - \nu_{12} \nu_{21}} = \frac{\nu_{21} E_1}{1 - \nu_{12} \nu_{21}} \quad (11)$$

$$Q_{33} = G_{I2} \quad (12)$$

$$m = \cos(\theta_j) \quad n = \sin(\theta_j) \quad (13)$$

Where j is number of the layer; h , \bar{Q}_{ij} and θ_j are respectively the thickness, the Hooke's elastic tensor and the fibers orientation of each layer.

By adopting the equilibrium conditions of the wooden, we have:

Along x – direction

$$\frac{dN_1(x)}{dx} = \tau(x)b_2 \quad (14)$$

where $\tau(x)$ is shear stress in the adhesive layer.

Along y – direction

$$\frac{dV_1(x)}{dx} = -[\sigma_n(x)b_2 + q] \quad (15)$$

where $V_1(x)$ is shear force applied in the wooden; $\sigma_n(x)$ is normal stress in the adhesive layer; q is the uniformly distributed load; and b_1 is width of wooden beam.

Moment equilibrium

$$\frac{dM_1(x)}{dx} = V_1(x) - \tau(x)b_2e \quad (16)$$

The equilibrium of the external composite (sika wrap) reinforcement along the x -, y – direction and moment equilibrium can also be written as

Along x – direction

$$\frac{dN_2(x)}{dx} = \tau(x)b_2 \quad (17)$$

Along y – direction

$$\frac{dV_2(x)}{dx} = \sigma_n(x)b_2 \quad (18)$$

Moment equilibrium

$$\frac{dM_2(x)}{dx} = V_2(x) - \tau(x)b_2 \frac{t_2}{2} \quad (19)$$

Where $V_2(x)$ is shear force applied in the external composite (sika wrap) reinforcement.

2.3 Mathematical formulation of the present model: Shear stress distribution along the composite–wooden interface

The shear stress in the adhesive can be expressed as follows

$$\tau(x) = K_s \Delta u(x) = K_s [u_2(x) - u_1(x)] \quad (20)$$

where K_s is shear stiffness of the adhesive per unit length and can be deduced as

$$K_s = \frac{\tau(x)}{\Delta u(x)} = \frac{\tau(x)}{\Delta u(x)/t_a} \frac{1}{t_a} = \frac{G_a}{t_a} \quad (21)$$

$\Delta u(x)$ is relative horizontal displacement at the adhesive interface; G_a is the shear modulus in the adhesive and t_a is the thickness of the adhesive.

Differentiating Eqs. (20), (1) and (2) with respect to x , respectively

$$\frac{d\tau(x)}{dx} = K_s \left[\left(A_{11} \frac{N_2(x)}{b_2} - D_{11} \frac{t_2}{2b_2} M_2(x) \right) - \left(\frac{y_1}{E_1 I_1} M_1(x) - \frac{N_1}{E_1 A_1} + \frac{t_1}{4G_1} \frac{d\tau_a}{dx} \right) \right] \quad (22)$$

Assuming equal curvature in the wooden beam and the composite plate, the relationship between the moments in the two adherends can be expressed as

$$M_1(x) = R M_2(x) \quad (23)$$

With

$$R = \frac{E_1 I_1 D_{11}}{b_2} \quad (24)$$

Moment equilibrium of the differential segment of the plated wooden beam in Fig. 3 gives

$$M_T(x) = M_1(x) + M_2(x) + N(x) \left(y_1 + t_a + \frac{t_2}{2} \right) \quad (25)$$

$M_T(x)$ is the applied moment and $N(x)$ is given as follows

$$N(x) = N_1(x) = N_2(x) = b_2 \int_0^x \tau(x) dx \quad (26)$$

The bending moment in wooden beam, expressed as a function of the total applied moment and the interfacial shear stress, is given as

$$M_1(x) = \frac{R}{R+1} \left[M_T(x) - b_2 \int_0^x \tau(x) \left(y_1 + t_a + \frac{t_2}{2} \right) dx \right] \quad (27)$$

And

$$M_2(x) = \frac{1}{R+1} \left[M_T(x) - b_2 \int_0^x \tau(x) \left(y_1 + t_a + \frac{t_2}{2} \right) dx \right] \quad (28)$$

The first derivative of the bending moment in each adherend gives

$$\frac{dM_1(x)}{dx} = \frac{R}{R+1} \left[V_T(x) - b_2 \tau(x) \left(y_1 + t_a + \frac{t_2}{2} \right) \right] \quad (29)$$

And

$$\frac{dM_2(x)}{dx} = \frac{1}{R+1} \left[V_T(x) - b_2 \tau(x) \left(y_1 + t_a + \frac{t_2}{2} \right) \right] \quad (30)$$

Differentiating Eq. (22)

$$\frac{d^2 \tau(x)}{dx^2} = \frac{G_a}{t_a} \left[\frac{A_{11}}{b_2} \frac{dN_2(x)}{dx} - D_{11} \frac{t_2}{2b_2} \frac{dM_2(x)}{dx} - \frac{y_1}{E_1 I_1} \frac{dM_1(x)}{dx} + \frac{1}{E_1 A_1} \frac{dN_1(x)}{dx} - \frac{t_1}{4G_1} \frac{d^2 \tau_a}{dx^2} \right] \quad (31)$$

Substitution of the shear forces (Eqs. (29) and (30)) and axial forces (Eq. (26)) into Eq. (31) gives the following governing differential equation for the interfacial shear stress

$$\frac{d^2 \tau(x)}{dx^2} - \frac{4G_a G_1}{4t_a G_1 + G_a t_1} \left[A_{11} + \frac{b_2}{E_1 A_1} + \frac{(y_1 + t_2/2)(e + t_a + t_2/2)}{E_1 I_1 D_{11} + b_2} b_2 D_{11} \right] \tau(x) + \frac{4G_a G_1}{4t_a G_1 + G_a t_1} \left[\frac{(y_1 + t_2/2)}{E_1 I_1 D_{11} + b_2} D_{11} \right] V_T(x) = 0 \quad (32)$$

For simplicity, the general solutions presented below are limited to loading which is either concentrated or uniformly distributed over part or the whole span of the beam, or both. For such loading, $d^2 V_T(x)/dx^2 = 0$, and the general solution to Eq. (32) is given by

$$\tau(x) = \Delta_1 \cosh(\xi x) + \Delta_2 \sinh(\xi x) + \frac{4G_a G_1 (y_1 + t_2/2) D_{11}}{\xi^2 (4t_a G_1 + G_a t_1) (E_1 I_1 D_{11} + b_2)} \left(\frac{L}{2} - x - a \right) q \quad (33)$$

where

$$\xi = \sqrt{\frac{4G_a G_1}{4t_a G_1 + G_a t_1} \left[A_{11} + \frac{b_2}{E_1 A_1} + \frac{(y_1 + t_2/2)(e + t_a + t_2/2)}{E_1 I_1 D_{11} + b_2} b_2 D_{11} \right]} \quad (34)$$

Δ_1 and Δ_2 are constant coefficients determined from the boundary conditions.

2.4 Mathematical formulation of the present model: Normal stress distribution along the composite- wooden interface

The normal stress in the adhesive can be expressed as follows

$$\sigma_n(x) = K_n \Delta w(x) = K_n [w_2(x) - w_1(x)] \quad (35)$$

where K_n is normal stiffness of the adhesive per unit length and can be deduced as

$$K_n = \frac{\sigma_n(x)}{\Delta w(x)} = \frac{\sigma_n(x)}{\Delta w(x)/t_a} \left(\frac{1}{t_a} \right) = \frac{E_a}{t_a} \quad (36)$$

$w_1(x)$ and $w_2(x)$ are the vertical displacements of adherend 1 (wooden beam) and 2 (composite

plate) respectively.

Differentiating Eq. (35) twice results in

$$\frac{d^2 \sigma_n(x)}{dx^2} = K_n \left[\frac{d^2 w_2(x)}{dx^2} - \frac{d^2 w_1(x)}{dx^2} \right] \quad (37)$$

Considering the moment – curvature relationships for the wooden beam to be strengthened and the external reinforcement, respectively

$$\frac{d^2 w_1(x)}{dx^2} = -\frac{M_1(x)}{E_1 I_1}, \quad \frac{d^2 w_2(x)}{dx^2} = -\frac{D_{11}' M_2(x)}{b_2} \quad (38)$$

Based on the equilibrium Eqs. (14)-(19), the governing differential equations for the deflection of adherends 1 and 2, expressed in terms of the interfacial shear and normal stresses, are given as follows:

Adherend 1

$$\frac{d^4 w_1(x)}{dx^4} = \frac{1}{E_1 I_1} b_2 \sigma_n(x) + \frac{y_1}{E_1 I_1} b_2 \frac{d\tau(x)}{dx} + \frac{q}{E_1 I_1} \quad (39)$$

Adherend 2

$$\frac{d^4 w_2(x)}{dx^4} = -D_{11}' \sigma_n(x) + D_{11}' \frac{t_2}{2} \frac{d\tau(x)}{dx} \quad (40)$$

Substitution of Eqs. (39) and (40) into the fourth derivation of the interfacial normal stress obtainable from Eq. (35) gives the following governing differential equation for the interfacial normal stress

$$\frac{d^4 \sigma_n(x)}{dx^4} + \frac{E_a}{t_a} \left[D_{11}' + \frac{b_2}{E_1 I_1} \right] \sigma_n(x) - \frac{E_a}{t_a} \left[D_{11}' \frac{t_2}{2} - \frac{y_1 b_2}{E_1 I_1} \right] \frac{d\tau(x)}{dx} + \frac{q E_a}{E_1 I_1 t_a} = 0 \quad (41)$$

The general solution to this fourth – order differential equation is

$$\begin{aligned} \sigma_n(x) = & e^{-\delta x} [\Delta_3 \cos(\delta x) + \Delta_4 \sin(\delta x)] + e^{\delta x} [\Delta_5 \cos(\delta x) + \Delta_6 \sin(\delta x)] \\ & - \frac{y_1 b_2 - D_{11}' E_1 I_1 t_2 / 2}{D_{11}' E_1 I_1 + b_2} \frac{d\tau(x)}{dx} - \frac{1}{D_{11}' E_1 I_1 + b_2} q \end{aligned} \quad (42)$$

For large values of x it is assumed that the normal stress approaches zero, and as a result $\Delta_3 = \Delta_4 = 0$. The general solution therefore becomes

$$\sigma_n(x) = e^{-\delta x} [\Delta_3 \cos(\delta x) + \Delta_4 \sin(\delta x)] - \frac{y_1 b_2 - D_{11}' E_1 I_1 t_2 / 2}{D_{11}' E_1 I_1 + b_2} \frac{d\tau(x)}{dx} - \frac{1}{D_{11}' E_1 I_1 + b_2} q \quad (43)$$

where

$$\delta = \sqrt[4]{\frac{E_a}{4t_a} \left(\frac{b_2}{E_1 I_1} + D_{11}' \right)} \quad (44)$$

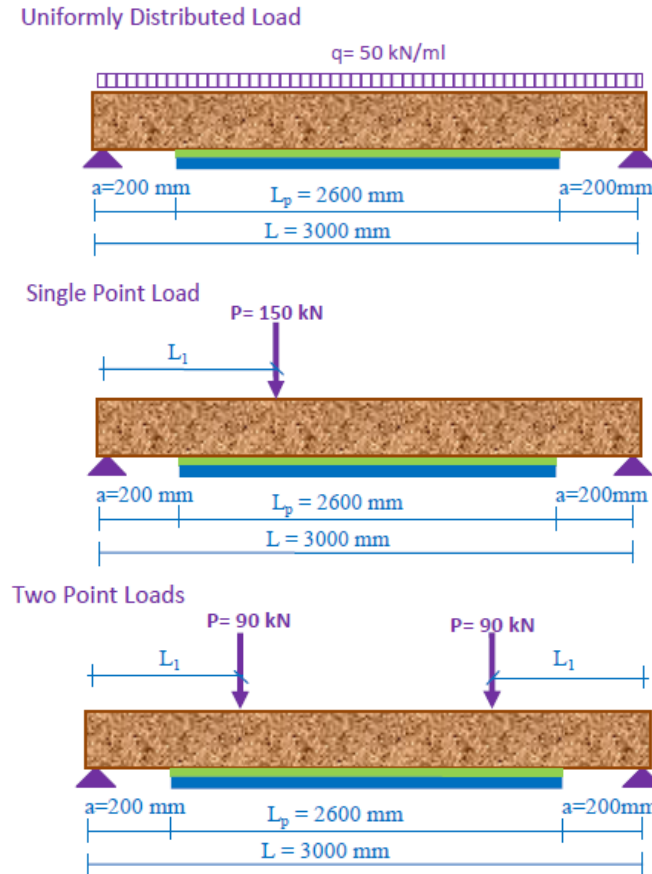


Fig. 4 Different loading cases for wooden beams reinforced by composite material

2.5 Application of boundary conditions

The same loads cases used by Tounsi (2006) is considered in the present method. A simply supported beam is investigated which is subjected to a uniformly distributed load and an arbitrarily positioned single point load as shown in Fig. 4.

This section derives the expressions of the interfacial shear and normal stresses for each load case by applying suitable boundary conditions.

Interfacial shear stress for a uniformly distributed load:

As is described by Tounsi (2006) the interfacial shear stress for this load case at any point is written as. The constants of integration need to be determined by applying suitable boundary conditions. The first boundary condition is applied at the bending moment at $x = 0$. Here, the moment at the plate end.

$M_f(0)$ and the axial force of either the wooden beam or sika wrap plate ($N_b(0) = N_f(0)$) are zero. As a result, the moment in the section at the plate curtailment is resisted by the beam alone and can be expressed as

$$M_1(0) = M_r(0) = \frac{qa}{2}(L - a) \quad (45)$$

Applying the above boundary condition in Eq. (30)

$$\frac{d\tau(x=0)}{dx} = -\frac{G_a y_1}{E_1 I_1 t_a} M_T(0) \tag{46}$$

By substituting Eq. (33) into (47), Δ_2 can be determined as

$$\Delta_2 = -\frac{q a}{2\xi} \frac{G_a y_1}{E_1 I_1 t_a} (L - a) + \frac{4G_a G_1 (y_1 + t_2 / 2) D'_{11}}{\xi^3 (4t_a G_1 + G_a t_1)(E_1 I_1 D'_{11} + b_2)} q \tag{47}$$

The second boundary condition requires zero interfacial shear stress at mid-span due to symmetry of the applied load. Δ_1 can therefore be determined as

$$\Delta_1 = \frac{a q}{2\xi} \frac{G_a y_1}{E_1 I_1 t_a} (L - a) \tanh\left(\frac{\xi L_p}{2}\right) - \frac{4G_a G_1 (y_1 + t_2 / 2) D'_{11} \cdot q}{\xi^3 (4t_a G_1 + G_a t_1)(E_1 I_1 D'_{11} + b_2)} \tanh\left(\frac{\xi L_p}{2}\right) \tag{48}$$

For practical cases $\frac{\xi L_p}{2} \gg 1$ and as a result $\tanh\left(\frac{\xi L_p}{2}\right) \approx 1$. So the expression for Δ_1 can be simplified to:

$$\Delta_1 = \frac{a q}{2\xi} \frac{G_a y_1}{E_1 I_1 t_a} (L - a) - \frac{4G_a G_1 (y_1 + t_2 / 2) D'_{11}}{\xi^3 (4t_a G_1 + G_a t_1)(E_1 I_1 D'_{11} + b_2)} q = -\Delta_2 \tag{49}$$

Substitution of Δ_1 and Δ_2 into Eq. (33) gives an expression for the interfacial shear stress at any point

$$\tau(x) = \frac{G_a y_1}{2E_1 I_1 t_a} (La - a^2) \frac{q e^{-\xi x}}{\xi} + \frac{4G_a G_1 (y_1 + t_2 / 2) D'_{11}}{\xi^2 (4t_a G_1 + G_a t_1)(E_1 I_1 D'_{11} + b_2)} \left[q\left(\frac{L}{2} - a - x\right) - \frac{q e^{-\xi x}}{\xi} \right] \tag{50}$$

$0 \leq x \leq L_p$

where q is the uniformly distributed load and x, a, L and L_p are defined in Fig. 2.

Interfacial shear stress for a single point load

The general solution for the interfacial shear stress for this load case is

$$\tau(x) = \begin{cases} \frac{G_a y_1}{\xi E_1 I_1 t_a} P a \left[1 - \frac{L_1}{L} \right] e^{-\xi x} \frac{q}{\xi} + \frac{4G_a G_1 (y_1 + t_2 / 2) D'_{11}}{\xi^2 (4t_a G_1 + G_a t_1)(E_1 I_1 D'_{11} + b_2)} P \left[1 - \frac{L_1}{L} - \cosh(\xi x) e^{-\xi(L_1 - a)} \right] & 0 \leq x \leq (L_1 - a) \\ \frac{G_a y_1}{\xi E_1 I_1 t_a} P a \left[1 - \frac{L_1}{L} \right] e^{-\xi x} \frac{q}{\xi} - \frac{4G_a G_1 (y_1 + t_2 / 2) D'_{11}}{\xi^2 (4t_a G_1 + G_a t_1)(E_1 I_1 D'_{11} + b_2)} \left[\frac{P L_1}{L} + P \sinh(\xi(L_1 - a)) e^{-\xi x} \right] & (L_1 - a) \leq x \leq L_p \end{cases} \tag{51}$$

$a > L_1$:

$$\tau(x) = \frac{G_a y_1}{\xi E_1 I_1 t_a} PL_1 \left[1 - \frac{a}{L} \right] e^{-\xi x} - \frac{4G_a G_1 (y_1 + t_2 / 2) D_{11}'}{\xi^2 (4t_a G_1 + G_a t_1)(E_1 I_1 D_{11}' + b_2)} \frac{PL_1}{L} \quad 0 \leq x \leq L_p \quad (52)$$

where P is the concentrated load.

Interfacial shear stress for two point loads

The general solution for the interfacial shear stress for this load case is

$a < L_1$:

$$\tau(x) = \begin{cases} \frac{G_a y_1}{\xi E_1 I_1 t_a} P a e^{-\xi x} + \frac{4G_a G_1 (y_1 + t_2 / 2) D_{11}'}{\xi^2 (4t_a G_1 + G_a t_1)(E_1 I_1 D_{11}' + b_2)} P [1 - \cosh(\xi x) e^{-\xi(L_1 - a)}] & 0 \leq x \leq (L_1 - a) \\ \frac{G_a y_1}{\xi E_1 I_1 t_a} P a e^{-\xi x} + \frac{4G_a G_1 (y_1 + t_2 / 2) D_{11}'}{\xi^2 (4t_a G_1 + G_a t_1)(E_1 I_1 D_{11}' + b_2)} P \sinh(\xi(L_1 - a)) e^{-\xi x} & (L_1 - a) \leq x \leq \frac{L_p}{2} \end{cases} \quad (53)$$

$a > b$:

$$\tau(x) = \frac{G_a y_1}{\xi E_1 I_1 t_a} PL_1 e^{-\xi x} \quad 0 \leq x \leq L_p$$

Interfacial normal stress: general expression for all three load cases

The constants Δ_3 and Δ_4 are determined using the appropriate boundary conditions and they are written as follow

$$\Delta_3 = \frac{E_a}{2\delta^3 E_1 I_1 t_a} [V_T(0) + \delta M_T(0)] - \frac{E_a b_2}{2\delta^3 t_a} \left(\frac{y_1}{E_1 I_1} - \frac{D_{11}' t_2}{2b_2} \tau(0) \right) + \frac{y_1 b_2 - D_{11}' E_1 I_1 t_2 / 2}{2\delta^3 (D_{11}' E_1 I_1 + b_2)} \left(\frac{d^4 \tau(0)}{dx^4} + \delta \frac{d^3 \tau(0)}{dx^3} \right) \quad (55)$$

$$\Delta_4 = -\frac{E_a}{2\delta^2 E_1 I_1 t_a} M_T(0) - \frac{y_1 b_2 - D_{11}' E_1 I_1 t_2 / 2}{2\delta^2 (D_{11}' E_1 I_1 + b_2)} \frac{d^3 \tau(0)}{dx^3} \quad (56)$$

The above expressions for the constants Δ_3 and Δ_4 have been left in terms of the bending moment $M_T(0)$ and shear force $V_T(0)$ at the end of the soffit plate. With the constants Δ_3 and Δ_4 determined, the interfacial normal stress can then be found using Eq. (44) for all three load cases.

Table 1 Property of the reinforcement material

Component	Young's modulus (MPa)	Poisson's ratio
Wood beam	$E_1 = 11750$	0.24
Adhesive layer	$E_a = 12800$	0.35
Sika Wrap	$E_2 = 165\ 000$	0.28
CFRP for honeycomb	$E_2 = 140\ 000$	0.28
Paper for honeycomb	$E_2 = 50$	0.4

3. Numerical results and discussions

3.1 Material used

A computer code based on the preceding equations was written to compute the interfacial stresses in a wooden beam bonded with a sika wrap plate and honeycomb sandwich plate. The composite material was selected in the present examples as a bonded plate. However, the analysis is equally applicable to other types of composite material. The material used for the present studies is an wooden beam bonded with composite plate. The beam is simply supported and subjected to a uniformly distributed load ($q = 50\text{ kN/ml}$). A summary of the material properties is given in Table 1 and the geometric characteristics of the beams are illustrated in Figs. 5-7.

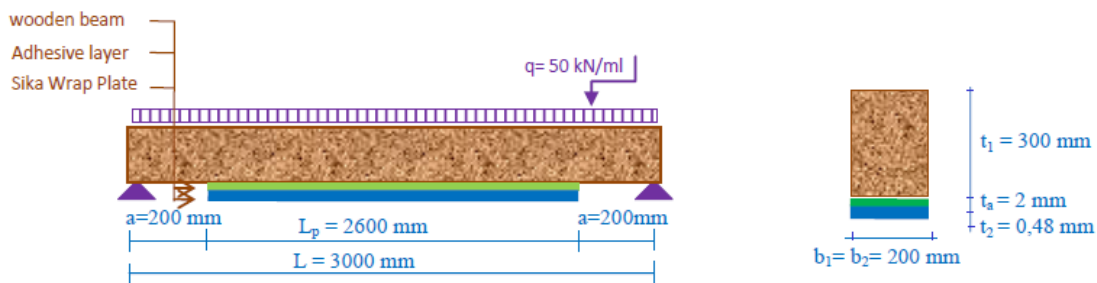


Fig. 5 Geometric characteristic of a simply supported wooden beam strengthened bonded with sika wrap plate

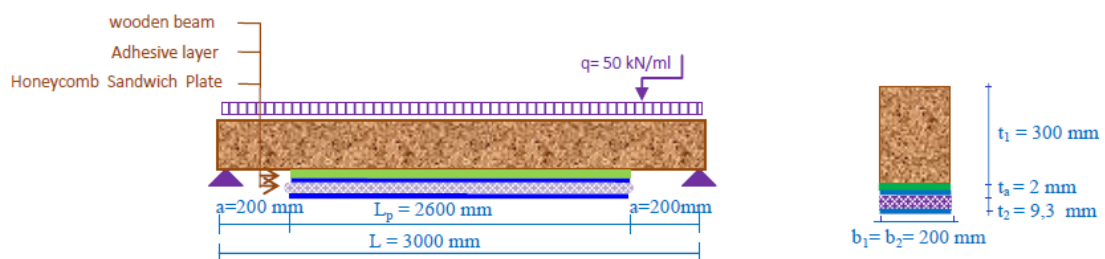


Fig. 6 Geometric characteristic of a simply supported wooden beam strengthened bonded with honeycomb sandwich plate

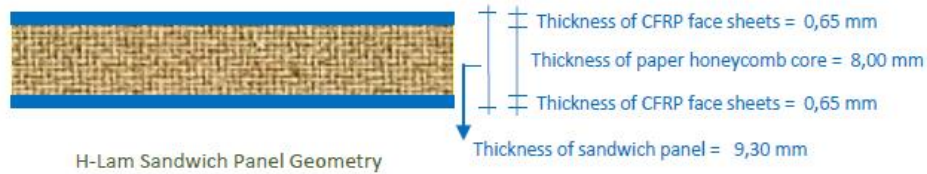


Fig. 7 Geometric characteristic of Honeycomb sandwich

3.2 Comparison with analytical solutions

A comparison of the interfacial shear and normal stresses from the different existing closed – form solutions and the present new solution is undertaken in this section. An wooden beam bonded with a composite soffit plate is considered. The beam is simply supported and subjected to a uniformly distributed load. A summary of the geometric and material properties is given in Table 1 and Figs. 5-7. The span of The wooden beam is 3000 mm, the distance from the support to the end of the plate is 200 mm and the uniformly distributed load is 50 kN/ml. The results of the peak interfacial shear and normal stresses are shows in Figs. 8 and 9 for the wooden beam strengthened by bonding composite plate. As it can be seen from the results, the peak interfacial stresses assessed by the present theory are smaller compared to those given by Tounsi (2006) solution. This implies that adherend shear deformation is an important factor influencing the adhesive interfacial stresses distribution. Figs. 8 and 9 the interfacial shear and normal stresses near the plate end for the example wooden beam bonded with a composite plate for the uniformly distributed load case. Overall, the predictions of the different solutions agree closely with each other. The interfacial normal stress is seen to change sign at a short distance away from the plate end.

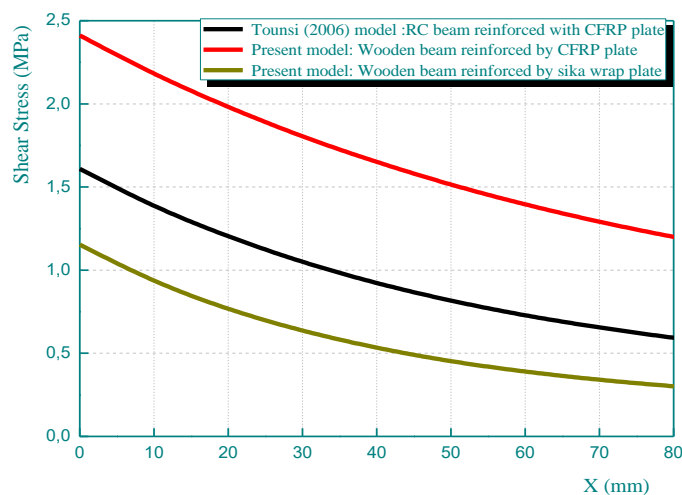


Fig. 8 Comparison of interfacial shear stress for composite plated wooden beam with the analytical results

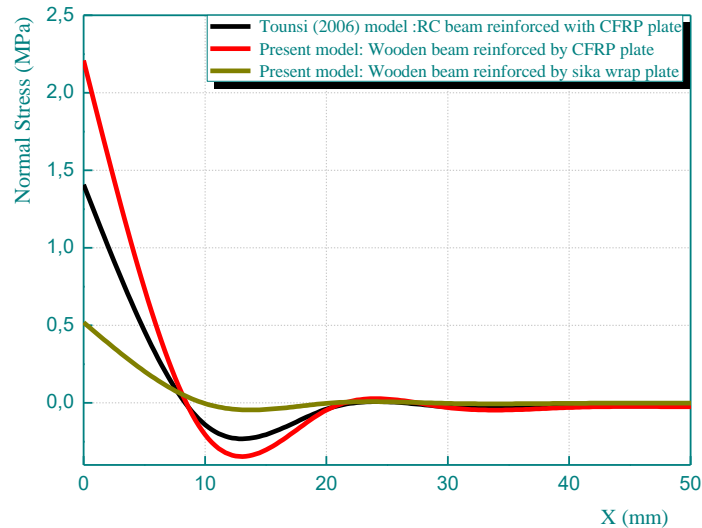


Fig. 9 Comparison of interfacial normal stress for composite plated wooden beam with the analytical results

The present analysis gives lower maximum interfacial shear and normal stresses than those predicted by Tounsi (2006), indicating that the inclusion of adherend shear deformation effect in the beam and soffit plate leads to lower values of τ_{\max} and σ_{\max} . However, the maximum interfacial shear and the normal stresses given by Tounsi (2006) method are higher than the results calculated by the present solution (wooden beam reinforced by Sika Wrap). This difference is due to the assumption used in the present theory which is in agreement with the beam theory (parabolic distribution of shear stresses through the depth of the beam). Hence, it is apparent that the adherend shear deformation reduces the interfacial stresses concentration and thus renders the adhesive shear distribution more uniform. The interfacial normal stress is seen to change sign at a short distance away from the plate end.

3.3 Effect of loading on the interfacial stress for the wooden beam

Table 2 shows the effect of loading on the interfacial stress for wooden beam strengthened by sika wrap plate, keeping the same geometry of the wooden beam as the reinforcing material, it is clear that the concentrated loads cause premature debonding of the composite at the end of the plate free end because of a concentration of the stresses higher than that of the distributed load, consequently we note that the wooden beam strengthened by sika wrap plate is stable in the case of a beam subjected to a distributed load compared to a concentrated load.

3.4 Efficiency of strengthening wooden beam by composite

Strain compatibility approach was used to predict the ultimate carrying capacity of the wooden beams. The results presented in Table 3 concerning the comparison of Load-deflection for wooden

beam strengthened by sika wrap plate, while varying the loading mode, namely a uniformly distributed load and a concentrated load in the middle of the beam, these results show: Linear elastic behaviour of the composite laminates was assumed based on the data provided by the manufacturer. Deflection of the beam was calculated using integration of the curvature along the span of each beam. Table 3 shows a good performance between an unreinforced beam and another reinforced by sika wrap plate for the two types of load, even more; it should be noted that a maximum deformation of 42% of the ultimate deformation values reported by the manufacturer was used as the upper limit to coincide with the maximum deformation measured on FRP laminates.

Table 2 Effect of loading on the interfacial stress for wooden beam strengthened by sika wrap plate

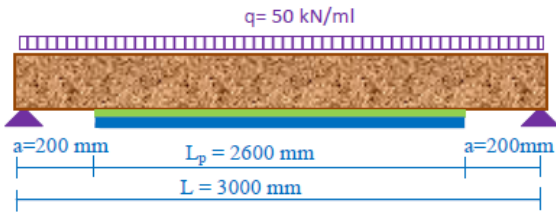
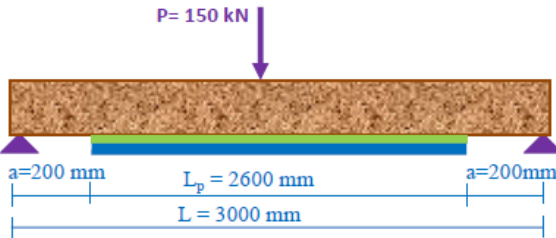
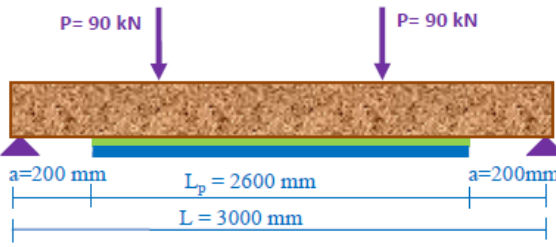
Configuration of the wooden beam for the three types of loading	Wooden beam reinforced by Sika Wrap plate	
	$\tau(x)$ (MPa)	$\sigma(x)$ (MPa)
 <p>Diagram showing a beam with a uniformly distributed load $q = 50 \text{ kN/ml}$. The beam length is $L = 3000 \text{ mm}$, with a reinforced section of length $L_p = 2600 \text{ mm}$. The distance from the beam ends to the start of the reinforced section is $a = 200 \text{ mm}$.</p>	1.1534	0.5197
 <p>Diagram showing a beam with a single concentrated load $P = 150 \text{ kN}$ at the center. The beam length is $L = 3000 \text{ mm}$, with a reinforced section of length $L_p = 2600 \text{ mm}$. The distance from the beam ends to the start of the reinforced section is $a = 200 \text{ mm}$.</p>	1.2563	0.5662
 <p>Diagram showing a beam with two concentrated loads $P = 90 \text{ kN}$ each. The beam length is $L = 3000 \text{ mm}$, with a reinforced section of length $L_p = 2600 \text{ mm}$. The distance from the beam ends to the start of the reinforced section is $a = 200 \text{ mm}$.</p>	1.2564	0.5606

Table 3 Comparison of Load-deflection for Wooden beam strengthened by sika wrap plate

Wooden beam reinforced by Sika Wrap plate	Load-deflection			
	Deflection (mm) for a $q = 50$ kN/ml	Maximum load q_{max} without deflection kN/ml	Deflection (mm) for a $P = 100$ kN	Maximum load P_{max} without deflection kN
Wooden beam "without strengthening"	$f = 10,024 \text{ mm}$	$q_{max} = 75,00$ kN/ml	$f = 10,66 \text{ mm}$	$P_{max} = 141,50 \text{ kN}$
Wooden beam strengthened by sika wrap plate "4-layer"	$f = 9,332 \text{ mm}$	$q_{max} =$ $80,21 kN/ml$	$f = 9,946 \text{ mm}$	$P_{max} = 150,00 \text{ kN}$

With this new strengthening system was used in the timber beam. In order to understand the effects of the strengthening of the wooden beam with sika wrap strips on the load-strain response of the beams, the equilibrium of the section was assumed in which the mechanical properties of the CFRP strips and the timber were considered. From the results presented, the main conclusions are as follows: The quality of timber is therefore crucial for the success of the bonding strengthening system. The flexural strengthened specimens showed an increase in their stiffness and strength when compared with the control specimen. And the wooden beam reinforcement system improves the load-carrying response of timber beams and the mechanical properties of the composites strips are fully used. Consequently, less stringent safety measures could be used in the design of this type of reinforcement.

3.5 Effect of FRP plate thickness

The thickness of the composite plate is an important design variable in practice. Figs. 10-12 shows the effect of the thickness of the Sika Wrap plate on the interfacial stresses. Here, five thickness values (2 layers (0.24 mm), 4 layers (0.48 mm), 6 layers (0.72 mm), 8 layers (0.96 mm) and 10 layers (1.2 mm)) are considered. It is shown that the level and concentration of interfacial stress are influenced considerably by the thickness of the Sika Wrap plate. The interfacial stresses increase as the thickness of Sika Wrap plate increases. Generally, the thickness of Sika Wrap plates used in practical engineering is small, compared with that of steel plate. Therefore, the fact of the smaller interfacial stress level and concentration should be one of the advantages of retrofitting by Sika Wrap plate compared with compared to another thick and rigid plate such as steel.

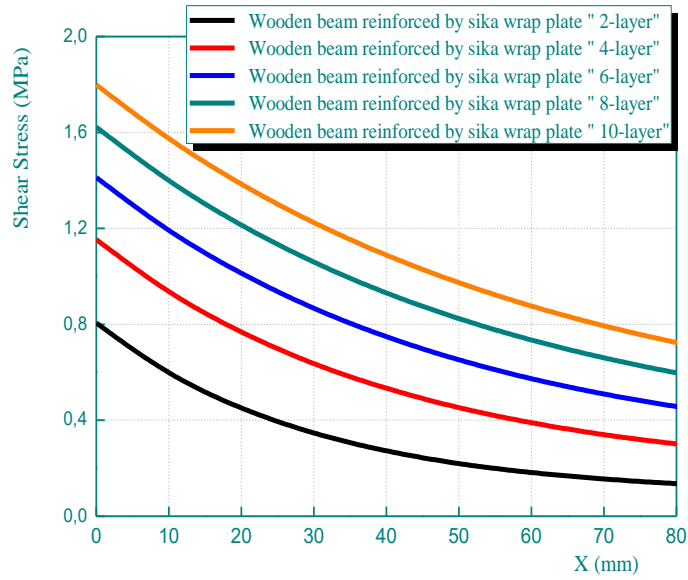


Fig. 10 Effect of plate thickness on interfacial shear stresses in strengthened wooden beam

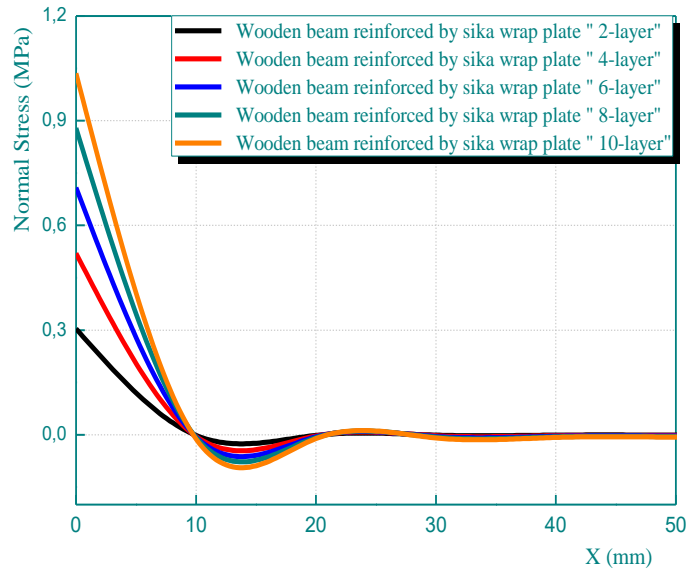


Fig. 11 Effect of plate thickness on interfacial normal stresses in strengthened wooden beam

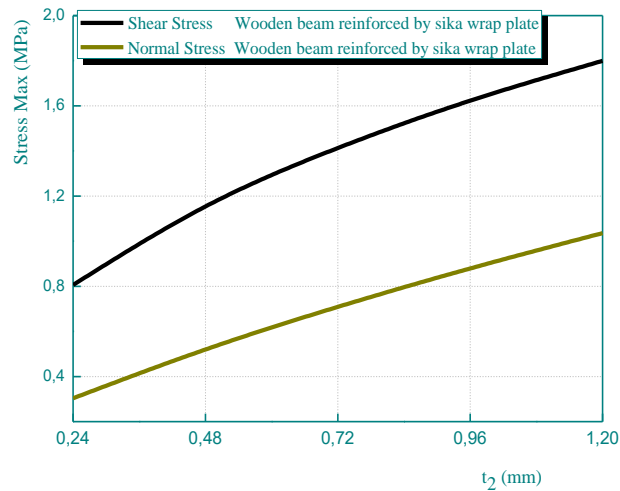


Fig. 12 Effect of plate thickness on interfacial stresses in strengthened wooden beam

3.6 Effect of FRP plate stiffness

Figs. 13 and 14 gives interfacial normal and shear stresses for the wooden beam bonded with a Sika Wrap plate, Sika Carbodur CFRP plate and Honeycomb sandwich plate, respectively, which demonstrates the effect of plate material properties on interfacial stresses. The length of the plate is $L_p=2600$ mm, and the thickness of the plate and the adhesive layer are both 4 mm. The results show that, as the plate material becomes softer (from Sika Carbodur and Honeycomb sandwich and then Sika Wrap), the interfacial stresses become smaller, as expected. This is because, under the same load, the tensile force developed in the plate is smaller, which leads to reduced interfacial stresses. The position of the peak interfacial shear stress moves closer to the free edge as the plate becomes less stiff.

3.7 Effect on plate length of the strengthened wooden beam region L_p

The influence of length of the strengthened beam region L_p appears in Fig. 15. It is seen that, as the plate terminates further away from the supports, the interfacial stresses increase significantly. This result reveals that in any case of strengthening, including cases where retrofitting is required in a limited zone of maximum bending moments at midspan, it is recommended to extend the strengthening strip as close as possible to the support lines.

3.8 Effect of elasticity modulus of adhesive layer

The adhesive layer is a relatively soft, isotropic material and has a smaller stiffness. The eight sets of Young's modules are considered here, which are 5; 6; 7; 8; 9; 10; 12 and 12.7 GPa. The Poisson's ratio of the adhesive is kept constant. The numerical results in Fig. 16 show that the property of the adhesive hardly influences the level of the interfacial stresses, whether normal or shear stress, but the stress concentrations at the end of the plate increase as the Young's modulus of the adhesive increases.

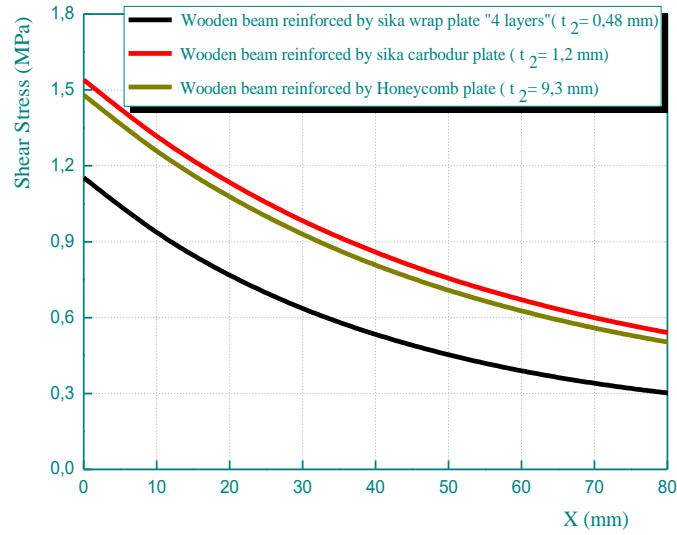


Fig. 13 Effect of plate stiffness on interfacial shear stresses in strengthened wooden beam

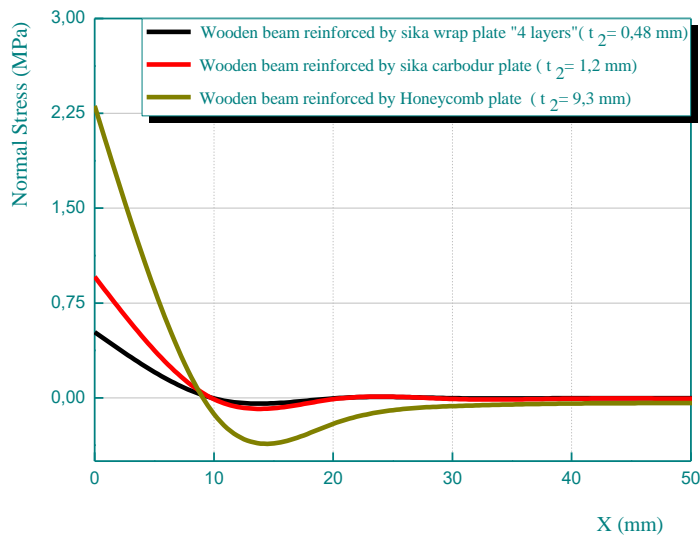


Fig. 14 Effect of plate stiffness on interfacial normal stresses in strengthened wooden beam

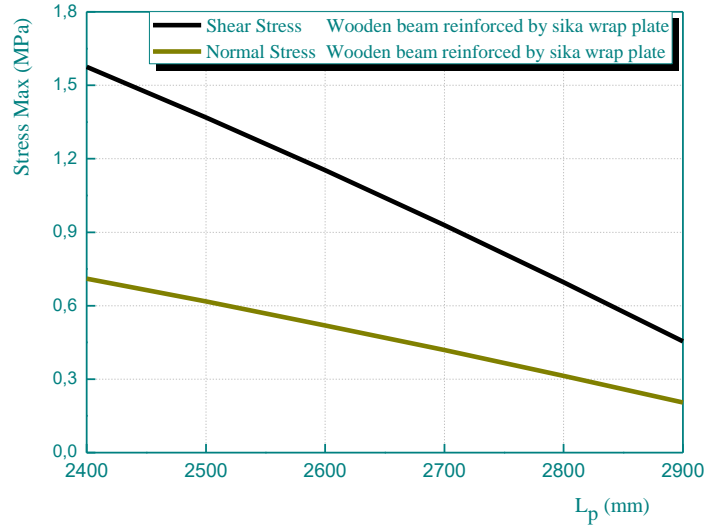


Fig. 15 Effect of plate length on edge stresses interfacial stresses in strengthened wooden beam

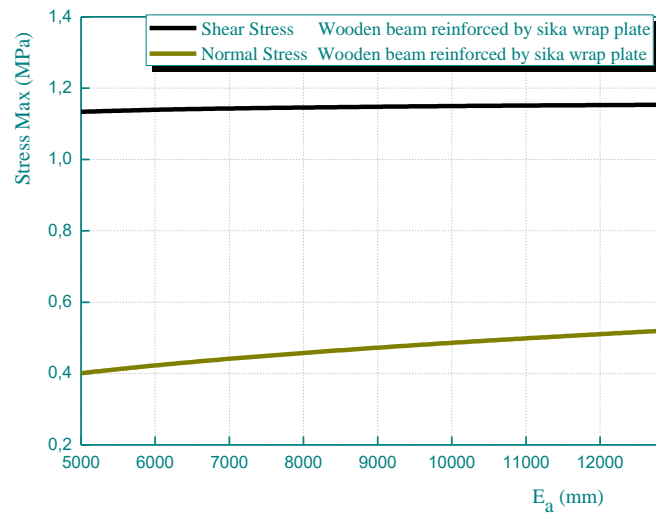


Fig. 16 Effect of adhesive moduli on interfacial stresses in strengthened wooden beam

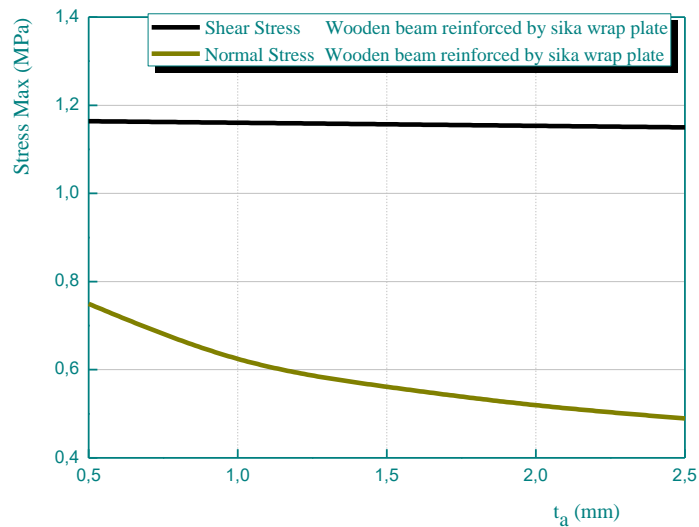


Fig. 17 Effect of adhesive layer thickness on interfacial stresses in strengthened wooden beam

3.9 Effect of the adhesive layer thickness

Fig. 17 shows the effects of the thickness of the adhesive layer on the interfacial stresses. It is seen that increasing the thickness of the adhesive layer leads to significant reduction in the peak interfacial stresses. Thus using thick adhesive layer, especially in the vicinity of the edge, is recommended.

4. Conclusions

This paper has been concerned with the prediction of interfacial shear and normal stresses in wooden beams retrofitted with externally advanced composite materials. Such interfacial stresses provide the basis for understanding debonding failures in such wooden beams and for development of suitable design rules. The salient features of this analysis include the consideration of the adherend shear deformations by assuming a parabolic shear stress through the thickness of both the wooden beam and bonded plate. The solution methodology is general in nature and may be applicable to the analysis of other types of composite structures. Numerical comparison between the existing solutions and the present new solution has been carried out, where this solution provides satisfactory predictions to the interfacial stress in the plated wooden beams. In the final part of this paper, extensive parametric studies were undertaken by using this solution for strengthened wooden beams with various ratios of design parameters. Observations were made based on the numerical results concerning their possible implications to practical designs.

The new solution is general in nature and may be applicable to all kinds of materials. As well as the proposed new solution was revealed to be quite easy to implement. The expertise acquired by the authors indicates that this new technique can be conjugated with other strengthening configurations. However, these new configurations should be optimized and a cost analysis would also be of benefit to designers.

Acknowledgments

This research was supported by the Algerian Ministry of Higher Education and Scientific Research (MESRS) as part of the grant for the PRFU research project n° A01L02UN140120200002 and by the University of Tiaret, in Algeria.

References

- Abdederak, R., Daouadji, T.H., Benferhat R. and Adim B. (2018), "Nonlinear analysis of damaged RC beams strengthened with glass fiber reinforced polymer plate under symmetric loads", *Earthq. Struct.*, **15** (2), 113-122. <https://doi.org/10.12989/eas.2018.15.2.113>.
- Abdelhady, H., *et al.* (2006), "Performance of reinforced concrete beams strengthened by hybrid FRP laminates", *Cement Concrete Compos.*, **28**(2006) 906-913. <https://doi:10.1016/j.cemconcomp.2006.07.016>.
- Abdelhak, Z., Lazreg Hadji, Z., Khelifa, T., Daouadji, T.H., E.A. and Adda Bedia, E.A. (2016), "Analysis of buckling response of functionally graded sandwich plates using a refined shear deformation theory", *Wind Struct.*, **22**(3), 291-305. <https://doi.org/10.12989/was.2016.22.3.291>.
- Abualnour, M., *et al.* (2019), "Thermomechanical analysis of antisymmetric laminated reinforced composite plates using a new four variable trigonometric refined plate theory", *Comput. Concrete*, **24**(6), 489-498. <https://doi.org/10.12989/cac.2019.24.6.489>.
- Adim, B., Daouadji, T.H., Rabahi, A., Benhenni, M., Zidour, M. and Boussad, A. (2018), "Mechanical buckling analysis of hybrid laminated composite plates under different boundary conditions", *Struct. Eng. Mech.*, **66**(6), 761-769. <https://doi.org/10.12989/sem.2018.66.6.761>.
- AlFurjan, M.S.H., *et al.* (2020), "A comprehensive computational approach for nonlinear thermal instability of the electrically FG-GPLRC disk based on GDQ method", *Eng. with Comput.*, <https://doi.org/10.1007/s00366-020-01088-7>.
- Alimirzaei, S., *et al.* (2019), "Nonlinear analysis of viscoelastic micro-composite beam with geometrical imperfection using FEM: MSGT electro-magneto-elastic bending, buckling and vibration solutions", *Struct. Eng. Mech.*, **71**(5), 485-502. <https://doi.org/10.12989/sem.2019.71.5.485>.
- Amara, K., Antar, K. and Benyoucef, S. (2019), "Hygrothermal effects on the behavior of reinforced-concrete beams strengthened by bonded composite laminate plates", *Struct. Eng. Mech.*, **69**(3), 327-334. <https://doi.org/10.12989/sem.2019.69.3.327>.
- Belbachir, N., *et al.* (2020), "Thermal flexural analysis of anti-symmetric cross-ply laminated plates using a four variable refined theory", *Smart Struct. Syst.*, **25**(4), 409-422. <https://doi.org/10.12989/sss.2020.25.4.409>.
- Benachour, A., Benyoucef, S., Tounsi, A. and Adda bedia, E.A. (2008), "Interfacial stress analysis of steel beams reinforced with bonded prestressed FRP plate", *Eng. Struct.*, **30**, 3305-3315. <https://doi.org/10.1016/j.engstruct.2008.05.007>.
- Benhenni, M.A., Daouadji, T.H., Abbes, B., Abbes, F., Li, Y. and Adim, B. (2019), "Numerical analysis for free vibration of hybrid laminated composite plates for different boundary conditions", *Struct. Eng. Mech.*, **70**(5), 535-549. <https://doi.org/10.12989/sem.2019.70.5.535>.
- Benhenni, M.A., Daouadji, T.H., Abbes, B., Adim, B., Li, Y. and Abbes, F. (2018), "Dynamic analysis for anti-

- symmetric cross-ply and angle-ply laminates for simply supported thick hybrid rectangular plates”, *Adv. Mater. Res.*, **7**(2), 83-103. <https://doi.org/10.12989/amr.2018.7.2.119>.
- Bensattalah, T., Zidour, M. and Daouadji, T.H. (2018), “Analytical analysis for the forced vibration of CNT surrounding elastic medium including thermal effect using nonlocal Euler-Bernoulli theory”, *Adv. Mater. Res.*, **7**(3), 163-174. <https://doi.org/10.12989/amr.2018.7.3.163>.
- Bourada, F., *et al.* (2020), “Stability and dynamic analyses of SW-CNT reinforced concrete beam resting on elastic-foundation”, *Comput. Concrete*, **25**(6), 485-495. <https://doi.org/10.12989/cac.2020.25.6.485>.
- Bousahla, A.A., *et al.* (2020), “Buckling and dynamic behavior of the simply supported CNT-RC beams using an integral-first shear deformation theory”, *Comput. Concrete*, **25**(2), 155-166. <https://doi.org/10.12989/cac.2020.25.2.155>.
- Boutaleb, S., *et al.* (2019), “Dynamic Analysis of nanosize FG rectangular plates based on simple nonlocal quasi 3D HSDT”, *Adv. Nano Res.*, **7**(3), 191-208. <https://doi.org/10.12989/amr.2019.7.3.191>.
- Chaabane, L.A., *et al.* (2019), “Analytical study of bending and free vibration responses of functionally graded beams resting on elastic foundation”, *Struct. Eng. Mech.*, **71**(2), 185-196. <https://doi.org/10.12989/sem.2019.71.2.185>.
- Chaded, A., Daouadji, T.H., Rabahi, A., Adim, B., Benferhat, R. and Fazilay, A. (2018), “A high-order closed-form solution for interfacial stresses in externally sandwich FGM plated RC beams”, *Adv. Mater. Res.*, **6**(4), 317-328. <https://doi.org/10.12989/amr.2017.6.4.317>.
- Chergui, S., Daouadji, T.H., Mostefa, H., Bougara, A., Abbas, B. and Amziane, S. (2019), “Interfacial stresses in damaged RC beams strengthened by externally bonded prestressed GFRP laminate plate: Analytical and numerical study”, *Adv. Mater. Res.*; **8**(3), 197-217. <https://doi.org/10.12989/amr.2019.8.3.197>.
- Chikr, S.S., *et al.* (2020), “A novel four-unknown integral model for buckling response of FG sandwich plates resting on elastic foundations under various boundary conditions using Galerkin’s approach”, *Geomech. Eng.*, **21**(5), 471-487. <https://doi.org/10.12989/gae.2020.21.5.471>.
- Daouadji, T.H. (2013), “Analytical Analysis of the Interfacial Stress in Damaged Reinforced Concrete Beams Strengthened by Bonded Composite Plates”, *Strength of Mater.*, **45**(5), 587-597. <https://doi.org/10.1007/s11223-013-9496-4>.
- Daouadji, T.H. (2017), “Analytical and numerical modeling of interfacial stresses in beams bonded with a thin plate”, *Adv. Comput. Design*, **2**(1), 57-69. <https://doi.org/10.12989/acd.2017.2.1.057>.
- Daouadji, T.H., Abdelaziz, H.H., Tounsi, A. and Adda bedia, E.A. (2013), “Elasticity Solution of a Cantilever Functionally Graded Beam”, *Appl. Compos. Mater.*, **20**(1), 1-15. <https://doi.org/10.1007/s10443-011-9243-6>.
- Daouadji, T.H., Benyoucef, S., Tounsi, A., Benrahou, K.H. and Adda bedia, E.A. (2008), “Interfacial Stresses Concentrations in FRP - Damaged RC hybrid Beams”, *Compos. Interfaces*, **15**(4), 425-440. <https://doi.org/10.1163/156855408784514702>.
- Daouadji, T.H., *et al.* (2019), “Flexural behaviour of steel beams reinforced by carbon fibre reinforced polymer: Experimental and numerical study”, *Struct. Eng. Mech.*, **72**(4), 409-419. <https://doi.org/10.12989/sem.2019.72.4.409>.
- Daouadji, T.H., Rabahi, A., Abbas, B. and Adim, B. (2016), “Theoretical and finite element studies of interfacial stresses in reinforced concrete beams strengthened by externally FRP laminates plate”, *J. Adhesion Sci. Technol.*, **30**(12), 1253-1280. <https://doi.org/10.1080/01694243.2016.1140703>.
- Draiche, K., *et al.* (2019), “Static analysis of laminated reinforced composite plates using a simple first-order shear deformation theory”, *Comput. Concrete*, **24**(4), 369-378. <https://doi.org/10.12989/cac.2019.24.4.369>.
- Guenaneche, B., Tounsi, A. and Adda Bedia, E.A. (2014), “Effect of shear deformation on interfacial stress analysis in plated beams under arbitrary loading”, *Adhesion & Adhesives*, **48**, 1-13. <https://doi.org/10.1016/j.ijadhadh.2013.09.016>.
- Hadj, B., *et al.* (2019), “Influence of the distribution shape of porosity on the bending FGM new plate model resting on elastic foundations”, *Struct. Eng. Mech.*, **72**(1), 823-832. <https://doi.org/10.12989/sem.2019.72.1.061>.
- Hugo, C.B., Carlos, C., David, C. and Noel, F. (2017), “Flexural Strengthening of Old Timber Floors with

- Laminated Carbon Fiber-Reinforced Polymers”, *J. Compos. Constr.*, 04016073 [https://doi:10.1061/\(ASCE\)CC.1943-5614.0000731](https://doi.org/10.1061/(ASCE)CC.1943-5614.0000731).
- Hussain, M., *et al.* (2020), “Computer-aided approach for modelling of FG cylindrical shell sandwich with ring supports”, *Comput. Concrete*, **25**(5), 411-425. <https://doi.org/10.12989/cac.2020.25.5.411>.
- Kaddari, M., *et al.* (2020), “A study on the structural behaviour of functionally graded porous plates on elastic foundation using a new quasi-3D model: Bending and Free vibration analysis”, *Comput. Concrete*, **25**(1), 37-57. <https://doi.org/10.12989/cac.2020.25.1.037>.
- Karami, M., *et al.* (2019), “Galerkin’s approach for buckling analysis of functionally graded anisotropic nanoplates/different boundary conditions”, *Eng. with Comput.*, **35**, 1297-1316. <https://doi.org/10.1007/s00366-018-0664-9>.
- Kliger, I.R., *et al.* (2016), “Wood-based beams strengthened with FRP laminates: improved performance with pre-stressed systems”, *European J. Wood Wood Products*, **74**, 319-330. <https://doi.org/10.1007/s00107-015-0970-5>.
- Liu, S., Yinzhi, Z., Qing Zheng, J.Z., Fengnian, J. and Hualin, F. (2019), “Blast responses of concrete beams reinforced with steel-GFRP composite bars”, *Structures*, 200-212. <https://doi.org/10.1016/j.istruc.2019.08.010>.
- Matouk, H., *et al.* (2020), “Investigation on hygro-thermal vibration of P-FG and symmetric S-FG nanobeam using integral Timoshenko beam theory”, *Adv. Nano Res.*, **8**(4), 293-305. <https://doi.org/10.12989/anr.2020.8.4.293>.
- Panjehpour, M., Farzadnia, N., Demirboga, R. and Ali, A. (2016), “Behavior of high-strength concrete cylinders repaired with CFRP sheets”, *J. Civil Eng. Management*, **22**(1), 56-64. <https://doi.org/10.3846/13923730.2014.897965>.
- Pello, L., Leire, G., Ignacio P. and José-Tomás S.J. (2020), “Flexural strengthening of low-grade reinforced concrete beams with compatible composite material: Steel Reinforced Grout (SRG)”, *Constr. Build. Mater.*, 235, article 117790. <https://doi.org/10.1016/j.conbuildmat.2019.117790>.
- Rabahi, A., Benferhat, R. and Daouadji, T.H. (2019), “Elastic analysis of interfacial stresses in prestressed PFGM-RC hybrid beams”, *Adv. Mater. Res.*, **7**(2), 83-103. <https://doi.org/10.12989/amr.2018.7.2.083>.
- Rabahi, A., Daouadji, T.H., Benferhat, R. and Adim, B. (2018), “Elastic analysis of interfacial stress concentrations in CFRP-RC hybrid beams: Effect of creep and shrinkage”, *Adv. Mater. Res.*, **6**(3), 257-278. <https://doi.org/10.12989/amr.2017.6.3.257>.
- Rabhi, M., *et al.* (2020), “A new innovative 3-unknowns HSDT for buckling and free vibration of exponentially graded sandwich plates resting on elastic foundations under various boundary conditions”, *Geomech. Eng.*, **22**(2), 119-132. <https://doi.org/10.12989/gae.2020.22.2.119>.
- Rabia, B., *et al.* (2018), “Analytical analysis of the interfacial shear stress in RC beams strengthened with prestressed exponentially-varying properties plate”, *Adv. Mater. Res.*, **7**(1), 29-44. <https://doi.org/10.12989/amr.2018.7.1.029>.
- Rabia, B., *et al.* (2019), “Effect of distribution shape of the porosity on the interfacial stresses of the FGM beam strengthened with FRP plate”, *Earthq. Struct.*, **16**(5), 601-609. <https://doi.org/10.12989/eas.2019.16.5.601>.
- Rahmani, M.C. (2020), “Influence of boundary conditions on the bending and free vibration behavior of FGM sandwich plates using a four-unknown refined integral plate theory”, *Comput. Concrete*, **25**(3), 225-244. <https://doi.org/10.12989/cac.2020.25.3.225>.
- Refrafi, S., *et al.* (2020), “Effects of hygro-thermo-mechanical conditions on the buckling of FG sandwich plates resting on elastic foundations”, *Comput. Concrete*, **25**(4), 311-325. <https://doi.org/10.12989/cac.2020.25.4.311>.
- Sahla, M., *et al.* (2019), “Free vibration analysis of angle-ply laminated composite and soft core sandwich plates”, *Steel Compos. Struct.*, **33**(5), 663-679. <https://doi.org/10.12989/scs.2019.33.5.663>.
- Shariati, A., *et al.* (2020), “Extremely large oscillation and nonlinear frequency of a multi-scale hybrid disk resting on nonlinear elastic foundation”, *Thin-Wall. Struct.*, **154**, 106840. <https://doi.org/10.1016/j.tws.2020.106840>.

- Shariati, A., *et al.* (2020), “Extremely large oscillation and nonlinear frequency of a multi-scale hybrid disk resting on nonlinear elastic foundations”, *Thin-Wall. Struct.*, **154**, 106840. <https://doi.org/10.1016/j.tws.2020.106840>.
- Smith, S.T. and Teng, J.G. (2002), “Interfacial stresses in plated beams”, *Eng. Struct.*, **23**(7), 857-871. [http://dx.doi.org/10.1016/S0141-0296\(00\)00090-0](http://dx.doi.org/10.1016/S0141-0296(00)00090-0).
- Tayeb, B. and Daouadji, T.H. (2020), “Improved analytical solution for slip and interfacial stress in composite steel-concrete beam bonded with an adhesive”, *Adv. Mater. Res.*, **9**(2), 133-153. <https://doi.org/10.12989/amr.2020.9.2.133>.
- Tounsi, A. (2006) , “Improved theoretical solution for interfacial stresses in concrete beams strengthened with FRP plate”, *Int. J. Solids Struct.*, **43**(14-15), 4154-4174. <https://doi.org/10.1016/j.ijsolstr.2005.03.074>.
- Tounsi, A., Daouadji, T.H., Benyoucef, S. and Adda bedia, E.A. (2008), “Interfacial stresses in FRP-plated RC beams: Effect of adherend shear deformations”, *Int. J. Adhesion Adhesives*, **29**, 313-351. <https://doi.org/10.1016/j.ijadhadh.2008.06.008>.
- Tounsi, A., *et al.* (2020), “A four variable trigonometric integral plate theory for hygro-thermo-mechanical bending analysis of AFG ceramic-metal plates resting on a two-parameter elastic foundation”, *Steel Compos. Struct.*, **34**(4), 511-524. <https://doi.org/10.12989/scs.2020.34.4.511>.
- Wang, Y.H., Yu, J., Liu, J.P., Zhou, B.X. and Chen, Y.F. (2020), “Experimental study on assembled monolithic steel-prestressed concrete composite beam in negative moment”, *J. Constr. Steel Res.*, **167**, 105667. <https://doi.org/10.1016/j.jcsr.2019.06.004>.
- Yehia, A. and Zaher, A. (2018), “Flexural behavior of FRP strengthened concrete-wood composite beams”, *Ain Shams Eng. J.* , **9**(4), 3419-3424. <https://doi.org/10.1016/j.asej.2018.06.003>.
- Yuan C., Chen, W., Pham, T.M. and Hao, H. (2019), “Effect of aggregate size on bond behaviour between basalt fibre reinforced polymer sheets and concrete”, *Compos. Part B: Eng.*, **158**, 459-474. <https://doi.org/10.1016/j.compositesb.2018.09.089>.
- Zidour, M., Si Tayeb, T., Bensattalah, T., Heireche, H., Benahmed, A. and Adda Bedia, E.A. (2020), “Mechanical buckling of FG-CNTs reinforced composite plate with parabolic distribution using Hamilton's energy principle”, *Adv. Nano Res.*, **8**(2), 135-148. <https://doi.org/10.12989/anr.2020.8.2.135>.